

# Spatiotemporal Contrastive Video Representation Learning

Rui Qian<sup>\*1,2,3</sup> Tianjian Meng<sup>\*1</sup> Boqing Gong<sup>1</sup> Ming-Hsuan Yang<sup>1</sup>  
 Huisheng Wang<sup>1</sup> Serge Belongie<sup>1,2,3</sup> Yin Cui<sup>1</sup>

<sup>1</sup>Google Research <sup>2</sup>Cornell University <sup>3</sup>Cornell Tech

## Abstract

We present a self-supervised Contrastive Video Representation Learning (CVRL) method to learn spatiotemporal visual representations from unlabeled videos. Inspired by the recently proposed self-supervised contrastive learning framework, our representations are learned using a contrastive loss, where two clips from the same short video are pulled together in the embedding space, while clips from different videos are pushed away. We study what makes for good data augmentation for video self-supervised learning and find both spatial and temporal information are crucial. In particular, we propose a simple yet effective temporally consistent spatial augmentation method to impose strong spatial augmentations on each frame of a video clip while maintaining the temporal consistency across frames. For Kinetics-600 action recognition, a linear classifier trained on representations learned by CVRL achieves 64.1% top-1 accuracy with a 3D-ResNet50 backbone, outperforming ImageNet supervised pre-training by 9.4% and SimCLR unsupervised pre-training by 16.1% using the same inflated 3D-ResNet50. The performance of CVRL can be further improved to 68.2% with a larger 3D-ResNet50 (4 $\times$ ) backbone, significantly closing the gap between unsupervised and supervised video representation learning.

## 1. Introduction

Representation learning is of crucial importance in computer vision tasks, and a number of highly promising recent developments in this area have carried over successfully from the static image domain to the video domain. Classic hand-crafted local invariant features (*e.g.*, SIFT [28]) for images have their counterparts (*e.g.*, 3D SIFT [34]) in videos. The temporal dimension of videos gives rise to key differences between them. Similarly, state-of-the-art neural networks for video understanding [39, 3, 19, 10, 9] often

<sup>\*</sup> The first two authors contributed equally. This work was conducted while Rui Qian worked at Google.

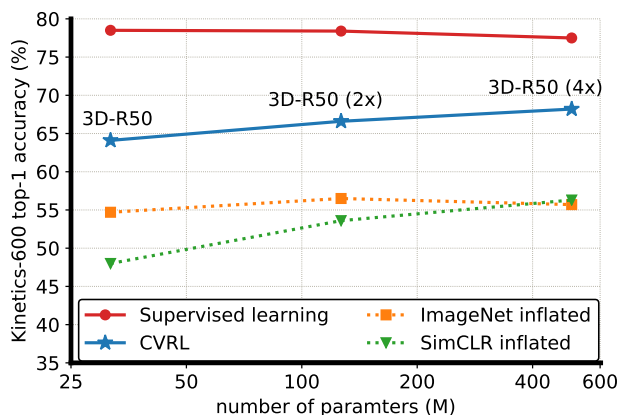


Figure 1. **Kinetics-600 top-1 linear classification accuracy** of different spatiotemporal representations. Our method CVRL outperforms same 3D inflated ResNet backbones from ImageNet supervised pre-training and SimCLR unsupervised pre-training, significantly closing the gap between unsupervised and supervised video representation learning.

extend 2D convolutional neural networks [21, 23] for images along the temporal dimension. More recently, unsupervised or self-supervised learning of representations from unlabeled visual data [20, 4, 17, 1] has gained momentum in the literature partially thanks to its ability to model abundantly available unlabeled data.

However, self-supervised learning gravitates to different dimensions in images and videos, respectively. It is natural to engineer self-supervised learning signals along the temporal dimension in videos. Examples abound, including models for predicting the future [36, 27, 18], changing temporal sampling rates [46], and sorting video frames or clips [26, 24, 45]. Meanwhile, in the domain of static images, some recent work [20, 4, 17, 1] that exploits the spatial dimensions has reported unprecedented performance on self-supervised image representation learning.

In this work, we show that the self-supervised signals in the spatial subspace of videos not only matter to video representation learning but also outperform the temporal cues.

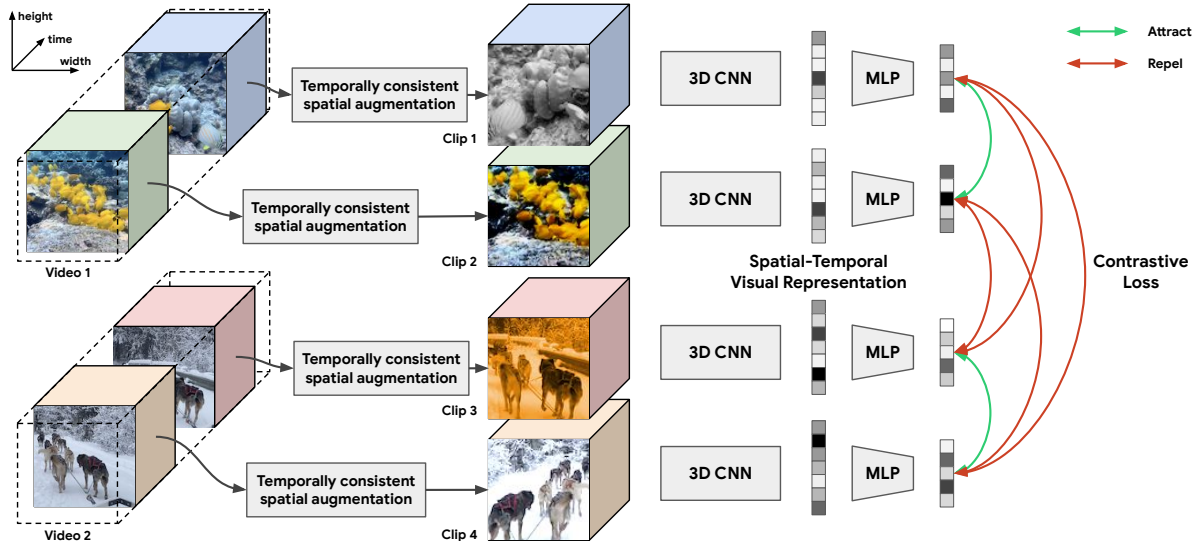


Figure 2. **Overview of the proposed self-supervised contrastive video representation learning (CVRL) framework.** From a short video, we randomly sample 2 clips with the same length. We then apply a temporally consistent spatial augmentation to each of the video clips and feed it to a 3D backbone with an MLP head. The contrastive loss is used to train the network to attract clips from the same video and repel clips from different videos in the embedding space.

We build a self-supervised framework of contrastive video representation learning (CVRL) upon SimCLR [4] in view of its simplicity and compelling performance in the image domain. As illustrated in Figure 2, this framework contrasts the similarity between two positive examples to those of negative pairs using the InfoNCE contrastive loss [30]. Since there is no label in self-supervised learning, we construct the positive pairs as two augmented video clips from the same short video. As a result, a plausible outcome of the contrastive self-supervised learning is that it separates all encoded videos into non-overlapping regions, such that any augmentations used in the training perturb an encoded video only within a small region in the representation space. We study both spatial and temporal augmentations and reveal that, when we combine them, it is vital to keep the spatial augmentations temporally consistent across all frames in a video clip. Finally, we evaluate the learned video representations in both the supervised learning setting by a linear protocol and the semi-supervised learning setting via fine-tuning the entire network following [4, 20, 17]. We next summarize our main findings.

**Our representations outperform existing ones.** To the best of our knowledge, all state-of-the-art methods on self-supervised learning for videos report lower accuracy than 3D inflated networks pre-trained on ImageNet [46, 15]. With our self-supervised video representations, on Kinetics-600 [2], we achieve 9.4% and 19.4% absolute gains in top-1 accuracy over the same 3D inflated ImageNet pre-trained networks in supervised and semi-supervised (using 1% of labeled data) evaluations, respectively.

**The self-supervised signals in the spatial subspace of videos do matter to video representations.** Spatial augmentations outperform temporal augmentations by 3.8% top-1 accuracy in a supervised linear evaluation. Combining the spatial augmentations with temporal augmentations yields 14.1% gain over spatial augmentations only. Adding the proposed temporal consistency for spatial augmentations further improves the performance by 10.4%.

**Our framework is less prone to overfitting.** Compared to supervised learning with the same networks on the same dataset, when networks overfit in supervised learning by increasing the network capacity ( $2\times$ ,  $4\times$ ), we do not observe overfitting in self-supervised learning (Figure 1).

**The main findings in SimCLR still hold in the video domain.** In our experiments, without SimCLR’s MLP projection head, the supervised linear evaluation result drops by almost 10%. The spatial augmentations optimized for self-supervised image learning yield higher accuracy than RandAugment [6], which is optimized for supervised ImageNet classification. A large batch size is important for achieving good performance. However, the performance could drop if the batch size is too large (2048 in our experiments). The optimizer [48] customized for large batches may be able to avoid the performance drop, and we leave it to future work.

Overall, we obtain our best result of 68.2% Kinetics-600 top-1 linear classification accuracy by combining the temporal augmentations and temporally consistent spatial augmentations, a larger network model ( $4\times$  of a vanilla 3D-ResNet [21]), a batch size as large as 1024, and a large number (300) of training epochs.

## 2. Related Work

**Self-supervised video representation learning.** It is natural to exploit the temporal dimension in self-supervised video representation learning. Some early work predicts the future on top of frame-wise representations [36]. More recent work learns from raw videos by predicting motion and appearance statistics [41] or encodings [27, 18]. Aside from predicting the future, another common approach is sorting frames or video clips [26, 45, 24, 11] along the temporal dimension. Yang *et al.* learn by maintaining consistent representations of different sampling rates [46]. Furthermore, videos can often supply multi-modal signals for cross-modality supervision, such as geometric cues [12], speech or language [37], and audio [25]. In contrast, we dive deep into the joint modeling of spatial and temporal dimensions, and we find that the the spatial subspace plays a more significant role than the temporal dimension for self-supervised video representation learning.

**Self-supervised image representation learning.** Some early work learns visual representations from unlabeled images via manually specified pretext tasks, for instance, the auto-encoding methods [32, 49, 50] that leverage contexts, channels, or colors. Other pretext tasks include but are not limited to relative patch location [7], jigsaw puzzles [29], and image rotations [13]. Interestingly, most of the pretext tasks can be integrated into a contrastive learning framework [20, 4, 47, 17, 30], which maintains relative consistency between the representations of an image and its augmented view. The augmentation could encompass various pretext tasks. Tian *et al.* study what makes a good view in this contrastive learning framework [38]. Clustering can also provide an effective addition to the framework [1]. Finally, it is worth noting that the recent wave of contrastive self-supervised learning shares a similar loss objective as instance discrimination [44].

**Videos as supervision for images and beyond.** Video can help supervise the learning of image representations [42, 31, 40, 15, 33], correspondences [43, 8], and robotic behaviors [35] thanks to its rich content about different views of objects and its motion and tracking cues. On the other hand, Girdhar *et al.* distill video representations from image representation networks [14].

## 3. Methodology

### 3.1. Video Representation Learning Framework

We build our self-supervised framework of contrastive video representation learning (CVRL) upon SimCLR [4] in view of its simplicity and compelling performance on learning image representations. Figure 2 shows an overview of our framework.

The core of this framework is an InfoNCE contrastive loss [30] applied on features extracted from augmented videos. Suppose we sample  $N$  videos per mini-batch and augment them, resulting in  $2N$  videos (the augmentation module is described in Section 3.3). Denote by  $z_i, z'_i$  the encoded representations of the two augmented versions of the  $i$ -th input video. The InfoNCE contrastive loss is defined as  $\mathcal{L} = \frac{1}{N} \sum_{i=1}^N \mathcal{L}_i$  and

$$\mathcal{L}_i = -\log \frac{\exp(\text{sim}(z_i, z'_i)/\tau)}{\sum_{k=1}^{2N} \mathbf{1}_{[k \neq i]} \exp(\text{sim}(z_i, z_k)/\tau)}, \quad (1)$$

where  $\text{sim}(\mathbf{u}, \mathbf{v}) = \mathbf{u}^\top \mathbf{v} / \|\mathbf{u}\|_2 \|\mathbf{v}\|_2$  is the inner product between two vectors after normalizing them onto a unit sphere,  $\mathbf{1}_{[\cdot]}$  is an indicator excluding from the denominator the self-similarity of the encoded video  $z_i$ , and  $\tau > 0$  is a temperature parameter. The loss allows the positive pair  $(z_i, z'_i)$  to attract mutually while they repel the other items in the mini-batch.

We construct other components of the framework as follows: (1) an encoder neural network maps an input video clip to its representation  $z$ , (2) spatiotemporal augmentations construct the positive pairs  $(z_i, z'_i)$  and the properties they induce, and (3) methods to evaluate the learned representations.

**Invariance, equivariance, and pretext tasks.** It is worth noting that the proposed contrastive framework for self-supervised learning can flexibly encompass a variety of tasks and objectives, whereas recent work [4, 20] focuses on representations that are invariant to certain data augmentations [33]. Take the equivariance to rotation for instance. Denote by  $R(\cdot)$  a rotation operation. We can enforce rotation-equivariance in the feature space by replacing the similarity function in Equation (1) by  $\text{sim}(R(z), z')$ , where  $z'$  is the feature map of the input rotated by  $R$ . In the same spirit, we may cast the pretext tasks reviewed in Section 2 into the contrastive loss. For instance, the colorization of an input was used as the predictive objective in [40], and the contrastive loss can instead use it for data augmentation or equivariance. Another example is the pretext task of sorting video frames or clips [26, 24, 45], which is straightforward to be included as an augmentation in our framework.

### 3.2. Video Encoder

We encode a video sequence using 3D-ResNets [21] as backbones. We expand the original 2D convolution kernels to 3D to capture spatiotemporal information in videos. The design of our 3D-ResNets mainly follows the “slow” pathway of the SlowFast network [10] with two modifications: (1) the temporal stride of 2 in the data layer, and (2) the temporal kernel size of 5 and stride of 2 in the first convolution layer. We also take as input a higher temporal resolution. Table 1 and Section 4.1 provide more details of the

Stage	Network	Output size $T \times S^2$
raw clip	-	$32 \times 224^2$
data	stride 2, $1^2$	$16 \times 224^2$
conv <sub>1</sub>	$5 \times 7^2, 64$ stride 2, $2^2$	$8 \times 112^2$
pool <sub>1</sub>	$1 \times 3^2$ max stride 1, $2^2$	$8 \times 56^2$
conv <sub>2</sub>	$\begin{bmatrix} 1 \times 1^2, 64 \\ 1 \times 3^2, 64 \\ 1 \times 1^2, 256 \end{bmatrix} \times 3$	$8 \times 56^2$
conv <sub>3</sub>	$\begin{bmatrix} 1 \times 1^2, 128 \\ 1 \times 3^2, 128 \\ 1 \times 1^2, 512 \end{bmatrix} \times 4$	$8 \times 28^2$
conv <sub>4</sub>	$\begin{bmatrix} 3 \times 1^2, 256 \\ 1 \times 3^2, 256 \\ 1 \times 1^2, 1024 \end{bmatrix} \times 6$	$8 \times 14^2$
conv <sub>5</sub>	$\begin{bmatrix} 3 \times 1^2, 512 \\ 1 \times 3^2, 512 \\ 1 \times 1^2, 2048 \end{bmatrix} \times 3$	$8 \times 7^2$
global average pooling		$1 \times 1^2$

Table 1. **Our video encoder: a 3D-ResNet50 backbone.** The input data has 16 frames (stride 2) in self-supervised pre-training and 32 frames (stride 2) in linear evaluation, semi-supervised learning and supervised learning.

network. The video representation is a 2048-dimensional feature vector. As suggested by SimCLR [4], we add an MLP with a hidden layer of 2048 dimension onto the backbone to obtain the encoded 128-dimensional feature vector  $z$  used in Equation (1). During evaluation, however, we discard the MLP and use the 2048-dimensional representation directly from the backbone to make the video encoder compatible with other supervised learning methods. We also experiment with  $2\times$  and  $4\times$  backbones, which multiply the number of filters in the network, including the backbone’s output feature dimension and all layers in MLP, by  $2\times$  and  $4\times$  accordingly.

### 3.3. Data Augmentation

The flexibility of our CVRL framework allows us to study a variety of desired properties, which are incorporated in the form of data augmentations. For the video representation learning, we focus on the augmentations in both temporal and spatial dimensions.

#### 3.3.1 Temporal Augmentation

We impose on the video representations an invariance-to-time property by a temporal augmentation within a short duration. The video encoder is desired to consider the following as a positive pair: what will be happening in the



Figure 3. **Illustration of temporally consistent spatial augmentation.** The middle row indicates frame-level spatial augmentations without temporal consistency which would be detrimental to the video representation learning.

future and what happened in the past. To this end, we apply a simple temporal augmentation method by sampling two clips with different start frames randomly from an input short video. We regard these two video clips as a positive pair. Therefore, the representations of them are mutually closer than the pairs of representations from different input videos, inducing the short-time invariance constraint on the learned representations. An ablation study in Table 2 verifies that temporal augmentation is indispensable in our framework for video representation learning.

#### 3.3.2 Temporally Consistent Spatial Augmentation

Spatial augmentation is widely used in both supervised learning and unsupervised learning in images. Although the question of how to apply strong spatial augmentations to videos remains open, a natural strategy is to utilize existing image-based spatial augmentation methods to the video frames one by one. However, this method could break the motion cues across frames. Spatial augmentation methods often contain some randomness such as random cropping, color jittering and blurring as important ways to strengthen their effectiveness. In videos, however, such randomness between consecutive frames, as shown in the middle row of Figure 3, could negatively affect the learning of representations along the temporal dimension. Therefore, we propose a simple yet effective approach to address this issue, by making the spatial augmentations consistent along the

---

**Algorithm 1:** Temporally consistent spatial augmentation procedure.

---

**Input:** Video clip  $V = \{f_1, f_2, \dots, f_M\}$  with  $M$  frames

**Resize:** Randomly resize to a scale  $S$  from  $[256, 320]$

**Crop:** Randomly crop a spatial region of  $224 \times 224$

**Flip:** Draw a flag  $F_f$  from  $\{0, 1\}$  with 50% on 1

**Jitter:** Draw a flag  $F_j$  from  $\{0, 1\}$  with 80% on 1

**Grey:** Draw a flag  $F_g$  from  $\{0, 1\}$  with 20% on 1

**for**  $k \in \{1, \dots, M\}$  **do**

$f'_k = \text{Resize}(f_k, \text{scale} = S)$

$f'_k = \text{Crop}(f'_k)$

$f'_k = \text{Flip}(f'_k)$  if  $F_f = 1$

$f'_k = \text{Color\_jitter}(f'_k)$  if  $F_j = 1$

$f'_k = \text{Greyscale}(f'_k)$  if  $F_g = 1$

$f'_k = \text{Gaussian\_blur}(f'_k)$

**end for**

**Output:** Augmented video clip  $V' = \{f'_1, f'_2, \dots, f'_M\}$

---

temporal dimension. With fixed randomness across frames, the 3D video encoder is able to better utilize spatiotemporal cues. This approach is validated by the experimental results in Table 2. Algorithm 1 presents a detailed description of our temporally consistent spatial augmentations.

### 3.4. Evaluation

We mainly evaluate the learned video representations by training a linear classifier on top of them for supervised human action recognition, namely, we fix the weights in the pre-trained video encoder. We also assess the learned representations by fine-tuning the entire video encoder network in a semi-supervised setting. Both evaluation methods follow the common practice in self-supervised image representation learning [4, 20]. Arguably, they are among the most representative tasks to evaluate the quality of the video representations, but they are by no means complete. We will study other evaluation protocols in future work.

## 4. Experiments

We conduct experiments on the Kinetics-600 dataset [2], which contains about 390k training videos and 29k validation videos belonging to 600 action classes<sup>1</sup>. The videos in Kinetics-600 have a duration of around 10 seconds, with 25 frames per second (*i.e.*, around 250 frames per video). We adopt the standard protocol for evaluating self-supervised representations. Specifically, we perform self-supervised pre-training of the video encoder on the Kinetics-600 training set by discarding all the labels. After that, we train a linear classifier on the training set by fixing all the weights in the pre-trained video encoder backbone network and report evaluation results on the validation set.

<sup>1</sup>Some videos become inaccessible over time. We use the version as of July 2020, which has 366k training videos and 27.8k validation videos.

## 4.1. Implementation Details

We use SGD as our optimizer with the momentum of 0.9. All models are trained with the mini-batch size of 1024. We linearly warm-up the learning rate in the first 5 epochs [16] followed by the scheduling strategy of half-period cosine learning rate decay [22]. We apply the proposed data augmentations in Algorithm 1 for the self-supervised pre-training. For the linear classifier training and semi-supervised training, we only use resizing, cropping and flipping. During testing, we densely sample 10 clips from each video and apply the 3-crop evaluation following [10]. The average of all prediction scores yields the final prediction. We present in Table 11 a study on the effect of different cropping strategies. Some task-specific implementation details are as follows.

**Self-supervised pre-training.** We sample two 16-frame clips with the temporal stride of 2 from each video for the self-supervised pre-training of video representations. The duration of a clip is 1.28 seconds out of around 10 seconds of a video. We use synchronized batch normalization to avoid information leakage or overfitting [4]. The temperature  $\tau$  is set to 0.1 in the InfoNCE loss for all experiments.

**Linear evaluation.** We evaluate the video representations using a linear classifier by fixing all the weights in the backbone network. During training, we sample a 32-frame clip with the temporal stride of 2 from each video (*i.e.*, a duration of 2.56 seconds) to train the linear classifier for 100 epochs with an initial learning rate of 32. We  $\ell_2$  normalize the feature representation before feeding it into the linear classifier.

**Semi-supervised learning.** Aside from the linear evaluation on the whole training set, we also evaluate our representations in a semi-supervised learning setting, namely, by fine-tuning the pre-trained encoder network on small subsets of Kinetics-600. We sample 6 and 60 videos from each class in the training set, forming two balanced subsets which are about 1% and 10% in size of the original training set, respectively. The evaluation set remains the same. We use the pre-trained backbones to initialize the network parameters and fine-tune all layers using an initial learning rate of 0.2 without warm-up. We train the model for 100 epochs on the 1% subset and 50 epochs on the 10% subset.

**Supervised learning.** To understand where our CVRL method stands, we also report the results of supervised learning. The setting for supervised learning is the same as linear evaluation except that we train the entire video encoder network from scratch for 200 epochs without feature normalization. We use the initial learning rate of 0.8 and a dropout rate of 0.5 following [10].

Temporal augmentation	Spatial augmentation	Temporal consistency	Accuracy top-1	Accuracy top-5
✓			33.0	57.6
	✓		36.8	62.6
✓	✓		50.9	75.4
✓	✓	✓	<b>61.3</b>	<b>84.2</b>

Table 2. **An ablation study on data augmentation.** All experiments are based on 100 epochs of self-supervised pre-training.

## 4.2. Experimental Results

**Ablation: data augmentation.** We conduct an ablation study on the proposed temporally consistent spatial augmentations in Table 2. We reach three major observations. First, both temporal and spatial augmentations are indispensable. Specifically, using both temporal and spatial augmentations yields 50.9% top-1 accuracy, significantly outperforming the same model pre-trained with temporal augmentations only (33.0%) or spatial augmentations only (36.8%). Second, the proposed temporally consistent module plays a critical role in achieving good performance. Adding temporal consistency further improves the top-1 accuracy to 61.3% (i.e., 10.4% improvement over the 50.9% by combining spatial and temporal augmentations without the temporal consistency). Third, the spatial augmentations, which are ignored to some degree in existing self-supervised video representation learning, not only matter, but also contribute more than the temporal augmentations.

**Comparison results.** We compare our CVRL method with two baselines: (1) inflating the 2D ResNets pre-trained on ImageNet to our 3D ResNets by duplicating it along the temporal dimension, called ImageNet inflated, and (2) SimCLR inflated by inflating the 2D ResNets pre-trained with SimCLR. In addition, the supervised learning serves as an upper bound of our method. As shown in Table 3, our CVRL outperforms the ImageNet inflated 3D encoder, which is pre-trained in a supervised manner, and the SimCLR inflated encoder trained in an unsupervised way, significantly closing the gap between self-supervised and supervised learning for videos. We also notice that larger backbones tend to overfit in supervised learning, while our self-supervised CVRL does not. We suspect that this might be due to the weaker data augmentation used in supervised learning. We will further study the overfitting issue of larger backbones in supervised learning in the future.

In the semi-supervised evaluation setting as shown in Table 4, our proposed CVRL surpasses all other baselines across different architectures and label fractions, especially when there is only 1% labeled data for fine-tuning, indicating that the advantage of our self-supervised CVRL is more profound when the labeled data is limited.

Method	Backbone	Accuracy	
		top-1	top-5
Supervised learning	3D-R50	78.5	94.1
	3D-R50 (2×)	78.4	93.7
	3D-R50 (4×)	77.5	92.8
ImageNet inflated	3D-R50	54.7	77.5
	3D-R50 (2×)	56.5	78.8
	3D-R50 (4×)	55.7	77.9
SimCLR inflated	3D-R50	48.0	71.5
	3D-R50 (2×)	53.6	76.1
	3D-R50 (4×)	56.3	78.2
CVRL	3D-R50	<b>64.1</b>	<b>85.8</b>
	3D-R50 (2×)	<b>66.6</b>	<b>87.5</b>
	3D-R50 (4×)	<b>68.2</b>	<b>88.0</b>

Table 3. **Main results on Kinetics-600.** CVRL shows its effectiveness by surpassing both ImageNet pre-training inflated weights and SimCLR inflated weights by large margins on various network architectures.

Method	Backbone	Top-1 Acc. ( $\Delta$ vs. Sup.)	
		Label fraction	
		1%	10%
Supervised learning	3D-R50	4.3	45.3
	3D-R50 (2×)	3.8	44.1
	3D-R50 (4×)	0.4	43.7
ImageNet inflated	3D-R50	17.3 (13.0 $\uparrow$ )	52.6 (7.3 $\uparrow$ )
	3D-R50 (2×)	19.7 (15.9 $\uparrow$ )	53.3 (9.2 $\uparrow$ )
	3D-R50 (4×)	19.5 (19.1 $\uparrow$ )	51.7 (8.0 $\uparrow$ )
SimCLR inflated	3D-R50	19.7 (15.4 $\uparrow$ )	48.3 (3.0 $\uparrow$ )
	3D-R50 (2×)	20.9 (17.1 $\uparrow$ )	52.5 (8.4 $\uparrow$ )
	3D-R50 (4×)	20.0 (19.6 $\uparrow$ )	55.5 (11.8 $\uparrow$ )
CVRL	3D-R50	<b>36.7 (32.4<math>\uparrow</math>)</b>	<b>56.1 (10.8<math>\uparrow</math>)</b>
	3D-R50 (2×)	<b>41.0 (37.2<math>\uparrow</math>)</b>	<b>59.4 (15.3<math>\uparrow</math>)</b>
	3D-R50 (4×)	<b>42.3 (41.9<math>\uparrow</math>)</b>	<b>61.0 (17.3<math>\uparrow</math>)</b>

Table 4. **Semi-supervised learning results on Kinetics-600.** When fine-tuning the entire network with only 1% and 10% labeled data, CVRL outperforms supervised learning, ImageNet pre-training and SimCLR pre-training significantly.

## 5. Discussion

**Do we need a deeper projection head?** SimCLR uses an MLP head with one hidden layer to project down the learned embedding [4]. In [5], more hidden layers lead to better results when the linear classifier for evaluation is applied to certain hidden layers of the MLP. We are also interested in the effect of more hidden layers in the MLP, but we choose to perform the linear evaluation on top of the backbone to make the comparison fair. As shown in Table 5, increasing the number of hidden layers leads to consistent improvement in accuracy. However, we should also be aware that one hidden layer incurs 4.2M additional parameters in the

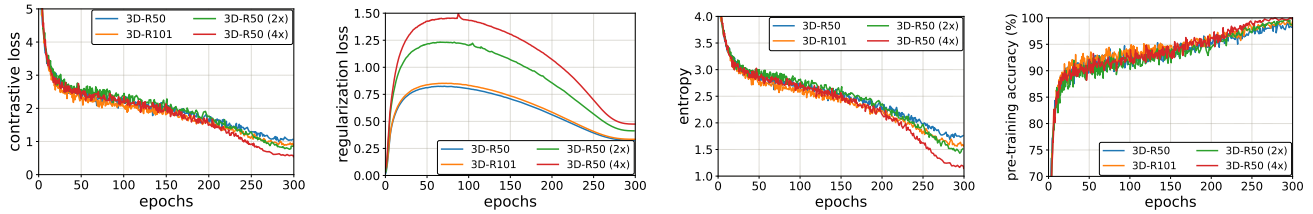


Figure 4. **Pre-training statistics.** Here we display four metrics: contrastive loss, regularization loss, contrastive entropy and pre-training accuracy. We use the weight decay of  $10^{-6}$  for the regularization loss.

Backbone	Hidden layers	Params	Accuracy	
			top-1	top-5
3D-R50	0	31.9M	52.6	77.5
	1	36.1M	61.3	84.2
	2	40.3M	62.2	84.6
	3	44.5M	<b>62.3</b>	<b>84.7</b>

Table 5. **Performance of different number of hidden layers in MLP** used in CVRL pre-training (100 epochs). “Params” indicates the total number of parameters in the pre-training network. Results of linear evaluation on top of the same backbone are reported.

network during pre-training. We choose to use only 1 hidden layer for all other experiments in our paper.

**Is going deeper beneficial?** In Table 3, we observe performance improvements brought by wider networks of 3D-ResNet50 (2 $\times$ ) and 3D-ResNet50 (4 $\times$ ). We are also interested in the effect of deeper networks. We experiment with 3D-ResNet101 and find that a deeper network is also beneficial for improving performance, as shown in Table 6. More detailed pre-training and fine-tuning statistics with respect to number of epochs for all backbones can be found in Figure 4 and Figure 5.

Method	Backbone	Accuracy	
		top-1	top-5
Supervised learning	3D-R50	78.5	94.1
	3D-R101	<b>80.0</b>	<b>94.8</b>
CVRL	3D-R50	63.9	85.7
	3D-R101	<b>65.0</b>	<b>86.7</b>

Table 6. **Performance of 3D-ResNet101.** 3D-ResNet101 brings consistent improvement in both supervised learning and CVRL over 3D-ResNet50 (300 epochs pre-training).

**Is large batch size always beneficial?** The batch size determines how many negatives pairs we use for each positive pair during training. Our experimental results show that a batch size of 1024 already achieves high performance. Switching to even larger batch sizes could negatively affect

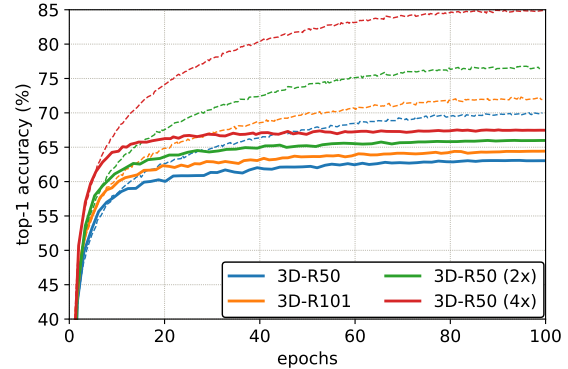


Figure 5. **Linear classification training (dashed-line) and evaluation (solid-line) top-1 accuracy** with 300 epochs of pre-training. Notice that the accuracy showed in this figure is calculated with a center-crop of  $224 \times 224$  resolution on a single clip for training and densely sampled 10 clips for evaluation.

the performance, as shown in Table 7. It would be interesting to study whether an improved optimizer [48] can better leverage larger batch sizes in the self-supervised setting.

Backbone	Batch size	Accuracy	
		top-1	top-5
3D-R50	256	60.4	83.1
	512	61.1	83.7
	1024	<b>61.3</b>	<b>84.2</b>
	2048	58.4	82.5

Table 7. **Performance of different batch sizes** used in CVRL pre-training (100 epochs). Linear evaluation results are reported.

**Are more frames in pre-training effective?** For our main results, we use clips of 16 frames in pre-training, while it is still worth studying the effect of using more frames. We experiment with 32 frames and results are shown in Table 8. Using 32 frames brings consistent improvement over 16 frames. However, the pre-training computation cost of the network in terms of FLOPs is also doubled. To make our method more computationally friendly, we choose to use the 16-frame input in all other experiments.

Backbone	# Frames	GFLOPs	Accuracy	
			top-1	top-5
3D-R50	16	45.6	61.3	84.2
	32	91.2	<b>61.8</b>	<b>84.5</b>
3D-R50 (2×)	16	172.8	64.5	86.0
	32	345.6	<b>65.2</b>	<b>86.4</b>

Table 8. **Performance of different input frames** used in CVRL pre-training (100 epochs). Pre-training FLOPs of the backbone (excluding MLP) and linear evaluation accuracy are reported.

**Is longer pre-training beneficial?** As shown in Table 9, we experiment with pre-training epochs varying from 100 to 500 and find consistent improvement with longer pre-training epochs. We also notice that CVRL’s performance starts to saturate after 300 epochs.

Backbone	# Pre-training epochs	Accuracy	
		top-1	top-5
3D-R50	100	61.3	84.2
	200	62.9	85.2
	300	63.9	85.7
	500	<b>64.1</b>	<b>85.8</b>
3D-R50 (2×)	100	64.5	86.0
	200	66.4	86.9
	300	66.4	87.2
	500	<b>66.6</b>	<b>87.5</b>
3D-R50 (4×)	100	64.7	86.2
	200	67.4	88.0
	300	<b>68.2</b>	<b>88.0</b>

Table 9. **Performance of different pre-training epochs.** The performance starts to saturate after 300 epochs.

**How does strong spatial augmentation in supervised learning perform in self-supervised CVRL?** We are interested in the performance of strong spatial augmentations that are widely used in supervised learning. We experiment with RandAugment [6] to randomly select 2 operators from a pool of 14. RandAugment with temporal consistency achieves 55.4% top-1 accuracy as shown in Table 10, which is lower than our temporally consistent spatial augmentation in Algorithm 1, implying that strong augmentations optimized for supervised image recognition do not necessarily perform as well in the self-supervised video representation learning.

**How does the cropping strategy affect evaluation results?** In Table 11, we present results of different evaluation cropping strategies. Using 10 clips improves the top-1 accuracy by 3% over 1-clip. The 3-crop evaluation on densely sampled 10 clips of  $256 \times 256$  resolution used in [10] further improves the performance by 0.5%.

Augmentation method	Accuracy	
	top-1	top-5
RandAugment w/ temporal consistency	55.4	79.6
Proposed	<b>61.3</b>	<b>84.2</b>

Table 10. **Performance of different spatial augmentations in pre-training (100 epochs).** Our proposed augmentation method outperforms RandAugment with temporal consistency.

Crop type	Scale	# Clips	Accuracy	
			top-1	top-5
Center-crop	224	1	60.6	82.1
Center-crop	224	10	63.6	84.5
Three-crop	256	10	<b>64.1</b>	<b>85.8</b>

Table 11. **Performance of different evaluation protocols.** A 3D-ResNet50 backbone with 500 epochs CVRL pre-training is used.

## 6. Conclusion

This work presents a contrastive video representation learning (CVRL) framework for learning spatiotemporal representations from unlabeled videos. Extensive experiments on Kinetics-600 demonstrate promising results and shed light on some key factors to fulfill the potential of this framework. In the future work, we plan to apply CVRL to a larger set of unlabeled videos and conduct transfer learning to downstream tasks.

## References

- [1] Mathilde Caron, Ishan Misra, Julien Mairal, Priya Goyal, Piotr Bojanowski, and Armand Joulin. Unsupervised learning of visual features by contrasting cluster assignments. *arXiv preprint arXiv:2006.09882*, 2020. 1, 3
- [2] Joao Carreira, Eric Noland, Andras Banki-Horvath, Chloe Hillier, and Andrew Zisserman. A short note about kinetics-600. *arXiv preprint arXiv:1808.01340*, 2018. 2, 5
- [3] Joao Carreira and Andrew Zisserman. Quo vadis, action recognition? a new model and the kinetics dataset. In *CVPR*, 2017. 1
- [4] Ting Chen, Simon Kornblith, Mohammad Norouzi, and Geoffrey Hinton. A simple framework for contrastive learning of visual representations. In *ICML*, 2020. 1, 2, 3, 4, 5, 6
- [5] Ting Chen, Simon Kornblith, Kevin Swersky, Mohammad Norouzi, and Geoffrey Hinton. Big self-supervised models are strong semi-supervised learners. *arXiv preprint arXiv:2006.10029*, 2020. 6
- [6] Ekin D Cubuk, Barret Zoph, Jonathon Shlens, and Quoc V Le. Randaugment: Practical automated data augmentation with a reduced search space. In *CVPR Workshops*, 2020. 2, 8
- [7] Carl Doersch, Abhinav Gupta, and Alexei A Efros. Unsupervised visual representation learning by context prediction. In *ICCV*, 2015. 3

- [8] Debidatta Dwibedi, Yusuf Aytar, Jonathan Tompson, Pierre Sermanet, and Andrew Zisserman. Temporal cycle-consistency learning. In *CVPR*, 2019. 3
- [9] Christoph Feichtenhofer. X3d: Expanding architectures for efficient video recognition. In *CVPR*, 2020. 1
- [10] Christoph Feichtenhofer, Haoqi Fan, Jitendra Malik, and Kaiming He. Slowfast networks for video recognition. In *ICCV*, 2019. 1, 3, 5, 8
- [11] Basura Fernando, Hakan Bilen, Efstratios Gavves, and Stephen Gould. Self-supervised video representation learning with odd-one-out networks. In *CVPR*, 2017. 3
- [12] Chuang Gan, Boqing Gong, Kun Liu, Hao Su, and Leonidas J Guibas. Geometry guided convolutional neural networks for self-supervised video representation learning. In *CVPR*, 2018. 3
- [13] Spyros Gidaris, Praveer Singh, and Nikos Komodakis. Unsupervised representation learning by predicting image rotations. *arXiv preprint arXiv:1803.07728*, 2018. 3
- [14] Rohit Girdhar, Du Tran, Lorenzo Torresani, and Deva Ramanan. Distinit: Learning video representations without a single labeled video. In *ICCV*, 2019. 3
- [15] Daniel Gordon, Kiana Ehsani, Dieter Fox, and Ali Farhadi. Watching the world go by: Representation learning from unlabeled videos. *arXiv preprint arXiv:2003.07990*, 2020. 2, 3
- [16] Priya Goyal, Piotr Dollár, Ross Girshick, Pieter Noordhuis, Lukasz Wesolowski, Aapo Kyrola, Andrew Tulloch, Yangqing Jia, and Kaiming He. Accurate, large mini-batch sgd: Training imagenet in 1 hour. *arXiv preprint arXiv:1706.02677*, 2017. 5
- [17] Jean-Bastien Grill, Florian Strub, Florent Alché, Corentin Tallec, Pierre H Richemond, Elena Buchatskaya, Carl Doersch, Bernardo Avila Pires, Zhaohan Daniel Guo, Mohammad Gheshlaghi Azar, et al. Bootstrap your own latent: A new approach to self-supervised learning. *arXiv preprint arXiv:2006.07733*, 2020. 1, 2, 3
- [18] Tengda Han, Weidi Xie, and Andrew Zisserman. Video representation learning by dense predictive coding. In *ICCV Workshops*, 2019. 1, 3
- [19] Kensho Hara, Hirokatsu Kataoka, and Yutaka Satoh. Can spatiotemporal 3d cnns retrace the history of 2d cnns and imagenet? In *CVPR*, 2018. 1
- [20] Kaiming He, Haoqi Fan, Yuxin Wu, Saining Xie, and Ross Girshick. Momentum contrast for unsupervised visual representation learning. In *CVPR*, 2020. 1, 2, 3, 5
- [21] Kaiming He, Xiangyu Zhang, Shaoqing Ren, and Jian Sun. Deep residual learning for image recognition. In *CVPR*, 2016. 1, 2, 3
- [22] Tong He, Zhi Zhang, Hang Zhang, Zhongyue Zhang, Junyuan Xie, and Mu Li. Bag of tricks for image classification with convolutional neural networks. In *CVPR*, 2019. 5
- [23] Andrew G Howard, Menglong Zhu, Bo Chen, Dmitry Kalenichenko, Weijun Wang, Tobias Weyand, Marco Andreetto, and Hartwig Adam. Mobilenets: Efficient convolutional neural networks for mobile vision applications. *arXiv preprint arXiv:1704.04861*, 2017. 1
- [24] Dahun Kim, Donghyeon Cho, and In So Kweon. Self-supervised video representation learning with space-time cubic puzzles. In *AAAI*, 2019. 1, 3
- [25] Bruno Korbar, Du Tran, and Lorenzo Torresani. Cooperative learning of audio and video models from self-supervised synchronization. In *Advances in Neural Information Processing Systems*, 2018. 3
- [26] Hsin-Ying Lee, Jia-Bin Huang, Maneesh Singh, and Ming-Hsuan Yang. Unsupervised representation learning by sorting sequences. In *ICCV*, 2017. 1, 3
- [27] William Lotter, Gabriel Kreiman, and David Cox. Deep predictive coding networks for video prediction and unsupervised learning. *arXiv preprint arXiv:1605.08104*, 2016. 1, 3
- [28] David G Lowe. Distinctive image features from scale-invariant keypoints. *IJCV*, 2004. 1
- [29] Mehdi Noroozi and Paolo Favaro. Unsupervised learning of visual representations by solving jigsaw puzzles. In *ECCV*, 2016. 3
- [30] Aaron van den Oord, Yazhe Li, and Oriol Vinyals. Representation learning with contrastive predictive coding. *arXiv preprint arXiv:1807.03748*, 2018. 2, 3
- [31] Deepak Pathak, Ross Girshick, Piotr Dollár, Trevor Darrell, and Bharath Hariharan. Learning features by watching objects move. In *CVPR*, 2017. 3
- [32] Deepak Pathak, Philipp Krahenbuhl, Jeff Donahue, Trevor Darrell, and Alexei A Efros. Context encoders: Feature learning by inpainting. In *CVPR*, 2016. 3
- [33] Senthil Purushwalkam and Abhinav Gupta. Demystifying contrastive self-supervised learning: Invariances, augmentations and dataset biases. *arXiv preprint arXiv:2007.13916*, 2020. 3
- [34] Paul Scovanner, Saad Ali, and Mubarak Shah. A 3-dimensional sift descriptor and its application to action recognition. In *ACM MM*, 2007. 1
- [35] Pierre Sermanet, Corey Lynch, Yevgen Chebotar, Jasmine Hsu, Eric Jang, Stefan Schaal, Sergey Levine, and Google Brain. Time-contrastive networks: Self-supervised learning from video. In *ICRA*, 2018. 3
- [36] Nitish Srivastava, Elman Mansimov, and Ruslan Salakhudinov. Unsupervised learning of video representations using lstms. In *ICML*, 2015. 1, 3
- [37] Chen Sun, Austin Myers, Carl Vondrick, Kevin Murphy, and Cordelia Schmid. Videobert: A joint model for video and language representation learning. In *ICCV*, 2019. 3
- [38] Yonglong Tian, Chen Sun, Ben Poole, Dilip Krishnan, Cordelia Schmid, and Phillip Isola. What makes for good views for contrastive learning. *arXiv preprint arXiv:2005.10243*, 2020. 3
- [39] Du Tran, Lubomir Bourdev, Rob Fergus, Lorenzo Torresani, and Manohar Paluri. Learning spatiotemporal features with 3d convolutional networks. In *ICCV*, 2015. 1
- [40] Carl Vondrick, Abhinav Shrivastava, Alireza Fathi, Sergio Guadarrama, and Kevin Murphy. Tracking emerges by colorizing videos. In *ECCV*, 2018. 3
- [41] Jiangliu Wang, Jianbo Jiao, Linchao Bao, Shengfeng He, Yunhui Liu, and Wei Liu. Self-supervised spatio-temporal

- representation learning for videos by predicting motion and appearance statistics. In *CVPR*, 2019. 3
- [42] Xiaolong Wang and Abhinav Gupta. Unsupervised learning of visual representations using videos. In *ICCV*, 2015. 3
- [43] Xiaolong Wang, Allan Jabri, and Alexei A. Efros. Learning correspondence from the cycle-consistency of time. In *CVPR*, 2019. 3
- [44] Zhirong Wu, Yuanjun Xiong, Stella X Yu, and Dahua Lin. Unsupervised feature learning via non-parametric instance discrimination. In *CVPR*, 2018. 3
- [45] Dejing Xu, Jun Xiao, Zhou Zhao, Jian Shao, Di Xie, and Yueting Zhuang. Self-supervised spatiotemporal learning via video clip order prediction. In *CVPR*, 2019. 1, 3
- [46] Ceyuan Yang, Yinghao Xu, Bo Dai, and Bolei Zhou. Video representation learning with visual tempo consistency. *arXiv preprint arXiv:2006.15489*, 2020. 1, 2, 3
- [47] Mang Ye, Xu Zhang, Pong C Yuen, and Shih-Fu Chang. Unsupervised embedding learning via invariant and spreading instance feature. In *CVPR*, 2019. 3
- [48] Yang You, Igor Gitman, and Boris Ginsburg. Large batch training of convolutional networks. *arXiv preprint arXiv:1708.03888*, 2017. 2, 7
- [49] Richard Zhang, Phillip Isola, and Alexei A Efros. Colorful image colorization. In *ECCV*, 2016. 3
- [50] Richard Zhang, Phillip Isola, and Alexei A Efros. Split-brain autoencoders: Unsupervised learning by cross-channel prediction. In *CVPR*, 2017. 3